ICARUS 5, 105–123 (1966)

The Ionospheric Model of the Venus Microwave Emission: An Obituary

RUSSELL G. WALKER

Harvard College Observatory and Office of Aerospace Research, Air Force Cambridge Research Laboratories Bedford, Massachusetts

AND

CARL SAGAN[1]

Harvard College Observatory and Smithsonian Astrophysical Observatory, Cambridge, Massachusetts

In the ionospheric model of Venus, the observed microwave radiation is attributed to free–free emission of electrons in a dense Cytherean ionosphere. The present paper discusses the mechanisms for formation of such a dense ionosphere, both in the original formulation of Jones and in later formulations which introduce holes in the ionosphere to achieve consistency with the observed radar reflectivities. Ionization by solar ultraviolet radiation and by the solar proton wind, as measured near Venus by Mariner 2, are considered, assuming that the Cytherean surface magnetic field strength is $\leq 10^{-3}$ gauss. Both sources of ionization are primarily effective at the level where the neutral particle density is $\sim 10^{11}$ cm^{-3}, somewhat above the level at which diffusive equilibrium is established. Three-body electron–ion recombination processes are ineffective at these densities. Radiative recombination is plausible only if all the N_2 at this level is converted to N by the Herzberg-Herzberg photodissociation mechanism. But the times for N to diffuse to dense levels where recombination to N_2 occurs are so much shorter than the time for Herzberg-Herzberg photodissociation on Venus, that N_2 must be a predominant atmospheric constituent at the level of the Cytherean ionosphere. If dissociative recombination therefore prevails, characteristic values of the electron density are $n_e \sim 10^6$ cm^{-3} over a region of 50-km thickness. If radiative recombination prevailed, $n_e \sim 10^8$ cm^{-3} would result, but even this is too small for the ionospheric model to be a valid explanation of the Venus microwave emission. The ionospheric model is accordingly rejected. We conclude that the observed microwave emission arises from the Cytherean surface.

Introduction

An extensive set of observations of the brightness temperature of Venus as a function of wavelength and phase have now been performed [see, e.g., Mayer (1963), Barrett and Staelin (1964), Pollack and Sagan (1965)]. Near inferior conjunction, temperatures of about 230°K are observed in the 8–13 μ infrared, rising to 350°K in the 4–8 mm region, and then to about 580°K at centimeter and decimeter wavelengths. A phase effect at centimeter wavelengths of the order of 50 K° now appears established, the dependence on phase being in the sense of an increase in temperature at phase angles removed from inferior conjunction.

Observations of the radar return from Venus at wavelengths of 68 cm, 43 cm, and 12.5 cm by Kotelnikov (1961), Pettengill *et al.* (1962), and Victor and Stevens (1961), respectively, have determined that the Cytherean reflectivity is some 10–12% the expected return from a perfectly conducting sphere of the same dimensions. Later measurements have confirmed these values. There is no compelling evidence for a wavelength dependence of reflectivity, and the radar results have been interpreted as indicating reflection from the solid surface of the planet.

Correlation of the variations from the

[1] Alfred P. Sloan Foundation Research Fellow.

mean value of the Astronomical Unit measured at 68 cm by Pettengill *et al.* (1962) with the 10.7-cm solar flux has been noted by Whipple (1962), while the same correlation with the 20-cm solar flux has been reported by Priester, Roemer, and Schmidt-Kaler (1962). The observed correlation is in the sense that an increase in solar flux is accompanied by a decrease in the value of the Astronomical Unit.

Three principal models have been proposed to explain the microwave observations. The greenhouse model (Sagan, 1960; Sagan and Pollack, 1966) and the aeolosphere model (Öpik, 1961) both attribute the 600°K radiation to emission from the planetary surface. In the ionospheric model (Jones, 1961; Sagan, Siegel, and Jones, 1961), the high brightness temperature is attributed to free–free transitions of electrons in a deep Cytherean ionosphere. Depending upon the particular model chosen, the atmospheric structure and surface conditions on Venus could be widely different. Critical discussions of the relative merits of these models have been given by Kellogg and Sagan (1961), Sagan and Kellogg (1963), and Sagan and Pollack (1966). In the present paper we attempt a critical appraisal of the ionospheric model.

Existing Ionospheric Models

The ionospheric models discussed by Jones (1961) and by Sagan, Siegel, and Jones (1961) consider the free–free emission of electrons in an isothermal layer at $T_e =$ 600°K. If the optical depth in the layer at 3 cm is about 2, a good fit to the microwave data is obtained. The dependence of the optical depth on the square of the wavelength renders the layer optically thick at wavelengths greater than 5 cm, and transparent for wavelengths less than 1 cm. To obtain the necessary opacity at 3 cm we require the integral of the square of the electron density through the layer to be of the order of 4×10^{25} cm^{-5} on the dark side of the planet. The phase variations reported at 8 mm can be reproduced if the electron density is two to five times greater on the sunlit side. A major difficulty with the ionospheric model is the maintenance of the high electron densities required, $n_e \sim 10^9$ to 10^{10} cm^{-3}. One must seek mechanisms for producing a very high ionization rate or else invoke extremely low values of the electron–ion recombination coefficient. Difficulties also arise in explaining the radar reflectivities since, if reflection arises from the surface, the high opacity of the ionospheric layer would cause almost complete absorption of the signal. To overcome this difficulty Kellogg and Sagan (1961) have suggested that there might be a "hole" in the ionosphere near the antisolar point where the electron density would be expected to decay during the long Venus night. Priester, Roemer, and Schmidt-Kaler (1962) have suggested that the radar reflectivity could be explained if the electrons were in clouds of $N_e \sim 10^9$ cm^{-3} covering one-fourth of the Cytherean surface with a mean density of $N_e \sim 10^8$ cm^{-3} in the regions between the clouds. Thus the radar return would be from the surface while the emission would arise from the electron clouds. The electron temperature on this model would be 800°K for an ionosphere 50 km thick. A similar suggestion has been made in two recent papers by Danilov and Yatsenko (1963).

In their first paper Danilov and Yatsenko conclude that the ionospheric model can be reconciled with the observations if radiative recombination of atomic ions is the dominant recombination process in the Venus ionosphere. However, to maintain the high electron densities observed on the dark side of the planet an unknown and enigmatic ionizing agent is postulated. No evidence is offered to support its presence. It is assumed that this agent is similar to that invoked to account for the observed ionization of the Earth's F layer over the polar regions during the long polar night. The radar data may be explained if it is assumed that 68-cm reflections result from the region of maximum electron density in the ionosphere, 43-cm radiation is totally reflected from the solid surface and attenuated by the ionosphere, and 12.5-cm radiation is partially absorbed upon reflection from the planetary surface.

In order to obtain the necessary transparency at 43 cm while still retaining the ionospheric reflection at 68 cm, the authors

require the electron temperature to be very high, $T_e \simeq 5000°K$. Such a high-temperature layer would exhibit a brightness temperature rapidly increasing with wavelength. To reduce this abrupt rise and thus bring the predicted brightness temperatures into rough agreement with those observed, an overlying low temperature ($T_e = 600°K$) layer is invoked. The *ad hoc* nature of these assumptions is quite striking.

In their second paper Danilov and Yatsenko propose a model similar to that of Priester, Roemer, and Schmidt-Kaler (1962). The lower ionosphere (they retain the two-layer concept) is porous—there are clouds of high electron density and interstitial regions of low electron density. The radar signals pass through the low-density regions unattenuated and are reflected from the surface. An optimum choice of parameters which yield a reasonably good fit to the observed spectrum is a temperature of 400°K at the surface, 1500°K in the hot layer, and 700°K in the cool layer. The surface reflectivity is taken to be 0.4, and the clouds of high electron density cover half of the planetary surface. An optical depth of 2 at $\lambda = 10$ cm is derived for both of these ionospheric layers.

Most recently, Kuzmin (1964) has proposed a range of ionospheric models with holes. He explicitly considers the effects of collisions with neutral particles in a somewhat unusual ionosphere, where the collision frequency greatly exceeds the free–free emission frequency so the absorption coefficient is wavelength-independent. The observed radar reflectivity will not necessarily be the true reflectivity of the surface, because of absorption in the ionosphere in the interstitial regions between the holes. If the holes cover only a small fraction of the disk of Venus, the true surface reflectivity must be very large. Thus, for a smooth surface with 20% ionospheric cover, an electron temperature of 1300°K, a surface temperature of 400°K, and a dielectric constant of about 5 are adequate. On the other hand, if the disk is 70% covered by an ionosphere, the electron temperature may be as low as 650°K, and the surface temperature, about 500°K; but the surface dielectric constant must now be about 15. As the total ionospheric cover becomes greater, the required values of the surface temperature rapidly exceed those required if the microwave emission arises mostly from the surface; at the same time, the dielectric constants become exceedingly large.

It is clearly difficult to achieve high electron densities in a region of high neutral particle densities. As we shall see below, neither solar electromagnetic radiation nor solar corpuscular radiation is likely to produce high electron densities in regions which have neutral particle densities in the range required by Kuzmin, who desires 10^{10} to 10^{11} collisions/sec. Such a collision frequency is characteristic of the terrestrial atmosphere near the surface. The corresponding atmospheric density on Venus is achieved just below the clouds (Sagan, 1962). But the Cytherean atmospheric rotational temperature at this depth is 300°K or less (Sagan, 1962), not the $\geq 600°K$ which must be the electron temperature for the ionospheric model to function. As the ionosphere is moved to deeper (and hotter) levels the situation is improved, but the whole point of the ionospheric model is to avoid a hot lower atmosphere. With no other source of ionization at hand, Kuzmin invokes either a primary cosmic-ray flux at Venus or a radioactive particle density below the Venus clouds several orders of magnitude larger than the corresponding values for Earth. Those models which place the ionosphere in the lower Cytherean atmosphere are too riddled with contradictions and improbabilities to be considered further here. Kuzmin's models which place the ionized layer in the upper Cytherean atmosphere give electron densities of the order of 2×10^9 cm^{-3}, in agreement with previous discussions.

There are two general objections to the ionospheric model besides the ones arising from economy of hypothesis. Drake (1962) has pointed out that as the wavelength of observation decreases, the brightness temperature observed in an optically thick ionosphere corresponds to greater and greater depths within the ionosphere. Unless the ionosphere is almost exactly isothermal—a circumstance of small probability—the

centimeter wavelength brightness temperature should be strongly wavelength-dependent, contrary to observation.

Secondly, an isothermal ionosphere becoming optically thin at about 1 cm should exhibit limb-brightening at that wavelength (Sagan, Siegel, and Jones, 1961). The Mariner 2 microwave radiometer channel at 19 mm showed, instead, limb-darkening (Barath *et al.*, 1963). Danilov (1964) has constructed a porous ionospheric model which yields, for wavelengths near 1 cm, limb-darkening over most of the disk and a sharp, thin intensity spike at the limb. While the topographical resolution of the Mariner 2 microwave experiment was small, it nevertheless was adequate to exclude most plausible ionospheric spikes.

But there seems little doubt that if sufficient ingenuity were employed, very complex models could be invented which have ionospheric holes strategically placed to simulate limb-darkening, and at the same time have closely isothermal interstitial material. The key property of all ionospheric models is the high electron density required. Since this is the most vulnerable feature of such models, it appears justified to examine in as much detail as possible what conditions exist in atmospheric regions appropriate to the formation of a Cytherean ionosphere. It is the purpose of this paper to discuss the mechanisms by which an ionosphere may be formed and maintained on Venus, with particular emphasis on ionization by solar protons, a mechanism first suggested by Jones (1961).

Basic Relations

The specific intensity $I(\nu, \theta)$ of radiation emerging at angle θ to the normal in a planetary atmosphere is given by the formal solution to the equation of radiative transfer,

$$I(\nu, \theta) = I_s(\nu, T_s)e^{-\tau/\mu} + \int_0^\tau I_a(\nu, \theta, \tau)e^{-\tau/\mu}\, d\tau/\mu, \quad (1)$$

where I_s is the specific intensity arising from the surface at emission temperature T_s, I_a is the intensity from the atmospheric layers, $\mu = \cos\theta$, and the optical depth τ is given by

$$\tau(\nu) = \int_{h_0}^{h} k(\nu, h)\, dh, \quad (2)$$

where h is the height in the atmosphere, and $k(\nu, h)$ the absorption cross section per unit volume. At radio frequencies the Rayleigh-Jeans approximation to the blackbody law may be used to express the intensity as

$$I(\nu, T) = (2h\nu^2/c^2)T, \quad (3)$$

where h is Planck's constant, and c is the velocity of light. Substitution of (3) into (1) and integration over all solid angles yields radio brightness temperatures,

$$T_B = 2\int_0^1 T(\mu)\, \mu\, d\mu, \quad (4)$$

or

$$T_B = 2T_sE_3(\tau_m) + 2\int_0^1 \int_0^{\tau_m} T(\tau)e^{-\tau/\mu}\, d\tau\, d\mu, \quad (5)$$

where τ_m refers to the total thickness of the atmospheric layers. For the special case of an isothermal atmospheric layer at a temperature T_a, Eq. (5) reduces to

$$T_B = 2T_sE_3(\tau_m) + T_a[1 - 2E_3(\tau_m)], \quad (6)$$

where $E_3(\tau)$ is the third exponential integral, tabulated, e.g., by Kourganoff (1952).

The absorption coefficient k which appears in Eq. (2) is given by Oster (1961) for free–free transitions of electrons. Adopting a value of 4.0 for the Gaunt factor yields, with the wavelength λ in centimeters,

$$k = 7.91 \times 10^{-23}\lambda^2(n_en_i/T_e^{3/2}), \quad (7)$$

where n_e is the electron density, n_i the ion density, and T_e the electron temperature. The optical depth from Eq. (2) is then

$$\tau(\lambda) = 7.91 \times 10^{-23}\lambda^2 \int_{h_0}^{h} n_e(h)n_i(h)T_e(h)^{-3/2}\, dh, \quad (8)$$

which, for the special case of an isothermal layer with $n_i = n_e$, is

$$\tau(\lambda) = 7.91 \times 10^{-23}\lambda^2T_e^{-3/2}\int_{h_0}^{h} n_e^2\, dh. \quad (9)$$

TABLE I[a]
VALUES OF $\int n_e^2\,dh$ FOR $\tau = 1$ AND $T_e \neq T_e(h)$

	$\int n_e^2\,dh$ at λ =						
T_e	0.5	1.0	3.4	10	21	43	68
600	7.42	1.86	1.61	1.86	4.21	1.00	4.01
800	11.4	2.86	2.48	2.86	6.50	1.55	6.18
1000	16.0	4.00	3.46	4.00	9.07	2.16	8.63
1500	29.3	7.34	6.36	7.34	16.7	3.97	15.8
2000	45.2	11.3	9.78	11.3	25.7	6.12	24.4
2500	63.1	15.8	13.6	15.8	35.8	8.54	34 1
3000	82.8	20.7	17.9	20.7	47.1	11.2	44.8
Column multiplier	$\times 10^{26}$	$\times 10^{26}$	$\times 10^{25}$	$\times 10^{24}$	$\times 10^{23}$	$\times 10^{23}$	$\times 10^{22}$

[a] $\int n_e^2\,dh$ in cm^{-5}; λ, cm; and T_e, °K.

Table I presents values of the integral of the square of the electron density required to achieve unit optical depth for a number of selected wavelengths and temperature as calculated from Eq. (9). It is obvious from the table that an increase in the temperature of the layer requires a substantial increase in the integrated electron density to achieve the same optical depth.

Consider now an atmosphere in hydrostatic equilibrium satisfying the perfect gas law. The pressure P at any level is determined by the relation

$$dP/P = -(mg/RT)\,dh, \tag{10}$$

where g is the local acceleration of gravity, m is the mean molecular weight in atomic mass units, T is the temperature in °K, and R is the universal gas constant [8.314×10^7 erg $gm^{-1}(K°)^{-1}$]. For the atmospheric models considered here it will be assumed that g and m remain constant for all heights h above the height h_b of the base or reference level.

For the case of an isothermal atmosphere at a temperature T, Eq. (10) integrates to

$$P(h) = P_b \exp[-(mg/RT)(h - h_b)], \tag{11}$$

where P_b is the pressure at the reference level h_b.

Integration of Eq. (10) for a temperature distribution of the form

$$T(h) = T_b + L(h - h_b) \tag{12}$$

and $L \neq 0$, yields for the pressure

$$P(h) = P_b \left[\frac{T_b}{T_b + L(h - h_b)}\right]^{(mg/RL)}, \tag{13}$$

where the constant L is the temperature gradient.

The reduced height of the atmospheric layer $w(h)$ is obtained from

$$w(h) = 22.4 \times 10^3 [P(h)/mg] \text{ cm-atm}, \tag{14}$$

where $P(h)$ is given by either Eq. (11) or Eq. (13) depending upon the model chosen. If we are interested in the reduced height for the ith atmospheric constituent, then $P(h)$ is replaced by the partial pressure $P_i(h)$.

The mean molecular weight m for any given atmospheric layer is given by

$$m = \sum_i n_i m_i / \sum_i n_i, \tag{15}$$

where n_i is the number density of the ith species of molecular weight m_i. The molecular weight is thus determined by the relative concentration of molecular and atomic species at the altitude h, and thus will be dependent upon the degree of dissociation at that altitude.

Of interest is the frequency with which particles of different types collide at any given level in the atmosphere. The collision frequency ν is determined by the mean

velocities $\bar{v}$ of the particles and the local mean free path x, through the relation

$$\nu = \bar{v}/x. \tag{16}$$

For a Maxwell-Boltzmann distribution of velocities

$$\bar{v} = (8RT/\pi m)^{1/2}, \tag{17}$$

and

$$x = (2^{1/2}\pi r^2 n)^{-1}; \tag{18}$$

r is the effective collision radius and is strongly dependent upon the types of colliding particles. For collisions between atoms and molecules in air r is of the order of 1.8×10^{-8} cm (Minzner and Ripley, 1957). Substitution of numerical values into Eq. (16) yields for collisions in air

$$\nu_n = 2.1 \times 10^{-11}(T/m)^{1/2} n_n \text{ sec}^{-1}, \tag{19}$$

where n_n is the total number density of neutral particles.

Ginzburg (1961) has discussed various collisional processes appropriate to free electrons in ionospheric layers. The total electron collisional frequency ν_e is given by

$$\nu_e = \nu_{e-n} + \nu_{e-i} + \nu_{e-e}, \tag{20}$$

where the subscript $(e\text{–}n)$ refers to collisions of electrons with neutral particles, $(e\text{–}i)$ to collisions with positive ions, and $(e\text{–}e)$ to electron–electron collisions. Substitution of numerical values into the relations derived by Ginzburg yields the following expressions:

$$\nu_{e-n} = 6.3 \times 10^{-9}(T/300)^{1/2} n_n \text{ sec}^{-1} \tag{21}$$

$$\nu_{e-i} = 29.7T^{-3/2} n_i[1 + 0.185 \ln (T/n^{1/3})] \text{ sec}^{-1} \tag{22}$$

$$\nu_{e-e} \simeq \nu_{e-i}. \tag{23}$$

Equation (22) holds for regions where the electron temperature T_e is equal to the local kinetic temperature T. For regions where $T_e \gg T$, Eq. (22) must be replaced by a more elaborate relation. For collisional frequencies involving positive ions, Ginzburg derives

$$\nu_{i-n} \simeq 1.5 \times 10^{-10} n_n (T/300)^{1/2} \text{ sec}^{-1} \tag{24}$$

and

$$\nu_{i-i} \simeq \frac{3.9 n_i}{T^{3/2}} \left(\frac{m_e}{m_i}\right)^{1/2} \ln\left(\frac{220T}{n^{1/3}}\right) \text{sec}^{-1}, \tag{25}$$

where m_e is the electron mass and m_i the mass of the positive ion.

For some purposes it will be convenient to express the number density $n(h)$ in terms of $w(h)$, the reduced height of the atmosphere. This may be accomplished by combining Eq. (14) with the equation of state giving

$$n(h) = 3.24 \times 10^{11} mgT^{-1} w(h). \tag{26}$$

The basic equations governing the time variation of the electron density n_e in an ionospheric layer are discussed, for example, by Mitra (1952) and by Nawrocki and Papa (1961). These relations depend upon the rates of processes which tend to increase the electron density (e.g., photoionization, photodetachment, collisional detachment, associative ionization); and of those processes which tend to decrease the electron density (e.g., electron–ion radiative recombination, dissociative recombination, electron attachment). At any given level in the atmosphere it is usually found that one set of processes effectively determines the electron density, and the very large number of other contributing reactions can be neglected. For the special case in which the electron production is by ionization and the decay of the electron density is controlled by recombination processes, the time variation of the electron density is given by

$$dn_e/dt = q - \alpha_e n_e^2, \tag{27}$$

where q is the ionization rate (electrons $\text{cm}^{-3}\ \text{sec}^{-1}$) and α_e is the effective recombination coefficient ($\text{cm}^3\ \text{sec}^{-1}$).

The decay of the electron density once the source of ionization has been removed is found from integration of Eq. (27) with $q = 0$, that is

$$n_e(t) = \frac{n_{e0}}{1 + n_{e0}\alpha_e(t - t_0)}, \tag{28}$$

where n_{e0} is the value of the electron density at $t = t_0$. The time interval Δt required for the electron density to fall to 1/2 of its initial value, obtained from Eq. (28) by setting $n_e(t) = (1/2)n_{e0}$, is

$$\Delta t = (n_e\alpha_e)^{-1}. \tag{29}$$

The quantity Δt is thus the mean lifetime of an electron.

At equilibrium in the layer, $dn_e/dt = 0$, and (27) reduces to

$$q = \alpha_e n_e^2 \tag{30}$$

or

$$n_e = (q/\alpha_e)^{1/2}. \tag{31}$$

Table II presents some values of q required by Eq. (30) to satisfy various combinations of α_e and n_e.

TABLE II

VALUES OF THE IONIZATION RATE q REQUIRED BY EQ. (30)

α_e (cm³ sec⁻¹)	q (cm⁻³ sec⁻¹) at n_e (cm⁻³) =					
	10^5	10^6	10^7	10^8	10^9	10^{10}
10^{-8}	10^2	10^4	10^6	10^8	10^{10}	10^{12}
10^{-10}	1	10^2	10^4	10^6	10^8	10^{10}
10^{-12}	10^{-2}	1	10^2	10^4	10^6	10^8
10^{-14}	10^{-4}	10^{-2}	1	10^2	10^4	10^6

PHOTOCHEMISTRY OF THE UPPER ATMOSPHERIC LAYERS

It is of interest to consider briefly what may be deduced concerning conditions in the upper atmosphere of Venus. Observations of the occultation of Regulus by de Vaucouleurs and Menzel (1960) indicate a pressure at the occultation level of 2.6 dynes cm^{-2}. These observations together with several observations pertaining to the temperature and scale height at this level have been discussed by Sagan (1962), who tentatively concluded that the following conditions exist at this level: $T_0 = 203$°K, $m_0 = 28.8$, and the scale height $H_0 = 6.8$ km. The value of the mean molecular weight m_0 is based upon a mixing ratio of α' CO_2 and $(1 - \alpha')$ N_2 below the occultation level, where $\alpha' \simeq 0.05$ and the CO_2 is 50% photodissociated at the occultation level. If the CO_2 abundance is smaller (Chamberlain, 1965) m_0 will decline very slightly. Substituting the above values into Eq. (14) and adopting $g = 870$ cm sec^{-2} we find the reduced height of the atmosphere above the occultation level to be $w_0(N_2 + CO_2) = 2.32$ cm-atm, $w_0(N_2) = 2.21$ cm-atm, and $w_0(CO_2) = 0.11$ cm-atm. From Eq. (26) the total number density is 9×10^{13} cm^{-3}, and from Eq. (19) the collision frequency $\nu_n = 5 \times 10^3$ sec^{-1}.

In the region above the occultation level photoionization and photodissociation will be important processes determining the upper atmospheric composition. For monochromatic radiation of frequency ν in a spectral region where the absorption by only one atmospheric constituent X is important, the optical depth in the zenith is given by

$$\tau_\nu(X) = k_\nu(X)w(X), \tag{32}$$

where $k_\nu(X)$ is the absorption coefficient in cm^{-1} and $w(X)$ is the reduced thickness of constituent X. In terms of the absorption cross section $\sigma_\nu(X)$, $k_\nu(X) = N_0\sigma_\nu(X)$ where N_0 is Loschmidt's number, 2.6875×10^{19} cm^{-3}. Substitution into Eq. (32) yields the reduced thickness required to achieve unit optical depth,

$$w_1(X) = 3.72 \times 10^{-20}[\sigma_\nu(X)]^{-1} \text{ cm-atm.} \tag{33}$$

Absorption cross sections for important atmospheric gases have been published by Nawrocki and Papa (1961), which is the source for all uncited cross sections and reaction rates in the following discussion.

Sagan (1961, 1962) has pointed out that CO_2 is dissociated on Venus by solar ultraviolet radiation according to

$$CO_2 + h\nu \rightarrow CO + O \ (\lambda < 1692 \text{ Å}), \tag{a}$$

where unit optical depth occurs near the occultation level [$w_1(CO_2) = 0.12$ cm-atm for $\sigma = 3.0 \times 10^{-19}$ cm^2]. This reaction proceeds if there is less than 0.03 cm-atm of O_2 above the occultation level, since the Schumann-Runge dissociation continuum reaches unit optical depth for this thickness at λ 1692.

Some possible reactions involving the products of (a) are

$$CO + O + Y \rightarrow CO_2 + Y \tag{b}$$

$$O + O + Y \rightarrow O_2 + Y \tag{c}$$

$$O + O_2 + Y \rightarrow O_3 + Y \tag{d}$$

$$O + O \rightarrow O_2 + h\nu \tag{e}$$

$$O_2 + h\nu \rightarrow O + O \ (\lambda 1250 - 1760 \text{ Å}) \tag{f}$$

$$O(^3P) + CO \rightarrow CO_2. \tag{g}$$

Reactions (b), (c), and (d) are three-body processes, while (e) is a two-body radiative process. Following Mitra (1952), we find that if N is the total particle number density, K the fraction of N which is the principle reactant (e.g., O in the above reactions), and $(1 - K)N$ the concentration of the third body, then the rate of recombination by three-body processes $q(3\text{-body}) = K^2(1 - K)N^3\beta$, where β is the three-body rate coefficient. The recombination rate by two-body processes is $q(2\text{-body}) = K^2N^2\alpha$, where α is the rate coefficient for two-body recombination. Thus one may write

$$q(3\text{-body})/q(2\text{-body}) = (1 - K)N(\beta/\alpha). \tag{34}$$

If we choose $K \ll 1$, which favors three-body processes, then from Eq. (34) it is seen that for $N \gg \alpha/\beta$ three-body processes will dominate and conversely for $N \ll \alpha/\beta$ two-body recombination will dominate. Rate coefficients for (c) and (d) given by Nawrocki and Papa (1961) are

$$\beta(\text{c}) = 3 \times 10^{-33}\ \text{cm}^6\ \text{sec}^{-1}$$
$$\beta(\text{d}) = 2 \times 10^{-34}\ \text{cm}^6\ \text{sec}^{-1}.$$

The rate coefficient for (e) has been estimated as $\alpha(\text{e}) = 10^{-16}\ \text{cm}^3\ \text{sec}^{-1}$ if both O atoms are in the ^3P state; if one is ^3P and the other ^1D the coefficient may be as high as $\alpha(\text{e}) = 10^{-14}\ \text{cm}^3\ \text{sec}^{-1}$. Coefficients for (b) have not been found; however, it is unlikely they will differ greatly from 10^{-33} to $10^{-34}\ \text{cm}^6\ \text{sec}^{-1}$. For $\beta = 10^{-33}\ \text{cm}^6\ \text{sec}^{-1}$ and $\alpha = 10^{-16}\ \text{cm}^3\ \text{sec}^{-1}$ we have $N \gg 10^{17}\ \text{cm}^{-3}$ as the condition for three-body processes to dominate. Since $N \simeq 10^{14}\ \text{cm}^{-3}$ at the occultational level we may conclude that three-body collisions are unimportant above the occultation level.

The rate q of photodissociation is determined by

$$q = \int f_\nu \sigma_\nu n\, d\nu \tag{35}$$

where f_ν is the solar photon flux, σ_ν is the cross section; and n is the number density. For reaction (a) the solar photon flux at $\lambda \leq 1692$ Å at Venus is 4×10^{12} photons $\text{cm}^{-2}\ \text{sec}^{-1}$, $\sigma \simeq 3 \times 10^{-19}\ \text{cm}^2$, and $n(CO_2) = 4.4 \times 10^{12}\ \text{cm}^{-3}$. Thus the rate at which O is formed is $q(\text{O}) = 5.3 \times 10^6$ atoms $\text{cm}^{-3}\ \text{sec}^{-1}$. If (e) proceeds rapidly the equilibrium concentration of O_2 will be determined by the reactions (a) and (f). The rate of depletion of O_2 is determined by absorption of $\lambda \leq 1750$ Å in the Schumann-Runge continuum. For this reaction the flux is 4×10^{12} photons $\text{cm}^2\ \text{sec}^{-1}$, $\sigma = 1.8 \times 10^{-17}\ \text{cm}^2$, and the rate $q(O_2) = 7.2 \times 10^{-5}\, n(O_2)$. In equilibrium $q(\text{O}) = q(O_2)$ or $n(O_2) = 7 \times 10^{10}\ \text{cm}^{-3}$; the corresponding reduced thickness for O_2 is 1.7×10^{-3} cm-atm. This represents an upper limit to the O_2 concentration above the occultation level. If (e) proceeds slowly the amount of O_2 will be less and a small equilibrium abundance of O will be maintained. If the assumptions inherent in the above analysis are correct, one expects to find no Schumann-Runge shielding of CO_2 and no appreciable amount of ozone above the occultation level. This analysis holds only for the sunlit side of the planet. During the long Venus night photodissociation ceases and decay of CO will proceed by (b) and (g), while the abundance of O_2 will probably be determined by a combination of (c), (d), and (e).

It is to be noted that solar radiation at $\lambda < 1026$ Å can photoionize O_2, the maximum cross section being $\sigma = 4 \times 10^{-18}\ \text{cm}^2$ at λ900. The reduced height for optical depth unity is about 10^{-2} cm-atm. Thus ionization can occur at the occulation level. Ionization of O can occur for $\lambda < 911$ Å with $\tau = 1$ at $w_1(\text{O}) = 10^{-2}$ cm-atm.

Solar radiation in the spectral region 796 − 200 Å will photoionize N_2. The mean value of the cross section for this region is $2 \times 10^{-7}\ \text{cm}^2$. At unit optical depth the reduced thickness is $w_1(N_2) = 2 \times 10^{-3}$ cm-atm. Due to the assumed great abundance of N_2, radiation in these wavelengths will not penetrate very deeply in the Cytherean atmosphere. Other absorptions occur in the Lyman-Birge-Hopfield bands (1450 − 1000 Å). Cross sections for the strongest bands are on the order of $10^{-20}\ \text{cm}^2$, yielding $w_1(\text{L-B-H}, N_2) \simeq 4$ cm-atm. Thus radiation of $\lambda > 800$ Å is essentially unattenuated by

N_2 in the upper atmosphere above the occultation level.

Dissociation of N_2 can occur by photoionization and dissociative recombination,

$$N_2 + h\nu \rightarrow N_2^+ + e \ (\lambda < 796 \text{ Å}) \quad \text{(h)}$$

$$N_2^+ + e \rightarrow N + N \quad \text{(i)}$$

or through the Herzberg-Herzberg predissociation mechanism (see Bates, 1954),

$$N_2(X^1\Sigma_g^+) + h\nu \rightarrow N_2(a^1\Pi_g), \quad \text{(j)}$$

(at 1200 – 1250 Å) followed by

$$N_2(a^1\Pi_g) \rightarrow N + N. \quad \text{(k)}$$

In the absence of other reactants the atomic nitrogen recombines by a three-body process,

$$N + N + Y \rightarrow N_2 + Y. \quad \text{(l)}$$

On Venus the rate for reaction (h) is $q(\text{h}) \sim 2.8 \times 10^{-7}\, n(N_2)$ while that for (j) would be $q(\text{j}) \sim 4 \times 10^{-12}\, n(N_2)$. At high altitudes where λ796 Å can penetrate and the number density is low, (h) will dominate, while at lower altitudes (j) will become important. Due to the slow rate of (l), $\beta(\text{l}) \simeq 10^{-27}$ cm^6 sec^{-1}, it is likely that nitrogen–oxygen reactions may produce small concentrations of NO and NO_2.

From recent balloon observations, Bottema, Plummer, and Strong (1964) estimate that the amount of water vapor above the cloud level is $\sim 10^{-2}$ gm cm^{-2}. Water vapor has a weak dissociation continuum at $\lambda <$ 1850 Å. The maximum cross section is at λ1650 where $w_1(H_2O) = 7 \times 10^{-3}$ gm cm^{-2}. Thus it is likely that H_2O is partially dissociated above the cloud level, in the absence of protection by O_2 or other absorbers.

Ionization Rate Due to the Solar Proton Wind

Jones (1961) has suggested that solar protons might provide a significant source of ionization on Venus. This suggestion will be considered in some detail here for an atmosphere having the required characteristics of the ionospheric model. In the following discussion it is assumed that Venus has a negligible magnetic field strength, an assumption consistent with but not proved by Mariner 2 magnetometer results.

The depth of penetration of protons into atmospheric gases has been studied by Cook, Jones, and Jorgensen (1953). For proton energies less than 76.5 keV the experimental data fit the empirical relation

$$R = 3.26E^{0.73}, \quad (36)$$

where E is the proton energy in keV and R is the range (in cm) of the protons in air at 1-mm pressure and 288°K. The reduced thickness of penetration, w, in cm-atm (at STP) is then

$$w = 4.06 \times 10^{-3}E^{0.73} \text{ cm-atm}. \quad (37)$$

Values of the proton flux and energy spectrum in interplanetary space as measured by Mariner 2 have been reported by Neugebauer and Snyder (1962). The pertinent data from their report are summarized in Table III together with the range w

TABLE III

Range and Energy of Interplanetary Protons

E/Q (volts)	v (km/sec)	E (keV)	w (cm-atm)	F (%)
516	314	0.517	0.0025	—
751	380	0.760	0.0033	18.3
1124	465	1.14	0.0045	22.5
1664	563	1.65	0.0059	30.5
2476	690	2.50	0.0079	19.9
3688	840	3.70	0.0106	0.3
5408	1016	5.42	0.0139	—
8224	1250	8.22	0.0190	—

calculated from Eq. (37) and the proton energy E calculated on the assumption that all particles measured were protons. The column headed F gives the fraction of the time the maximum of the spectral flux occurred at this value of the energy-to-charge ratio, E/Q. A typical value for the particle density during periods of no geomagnetic storms was given as 2.5 protons cm^{-3} at $E/Q = 1124$ volts. For the purposes of the following discussion the values of the proton flux, $n_p v$, in Table IV will be adopted as representative of average values at the top of the Cytherean atmosphere. This spectrum assumes $n_p = 4.0$ protons cm^{-3} for 751 volts $\leq E/Q \leq 2476$ volts, $n_p = 0.4$ cm^{-3} for $E/Q = 3688$ volts, and $n_p = 0$ outside these limits. These values of n_p were obtained from

the Mariner 2 data, and adjusted to the Venus–Sun distance by direct scaling of the solar wind model of Brandt (1962). It is believed that the adopted proton spectrum represents a reasonable upper limit to the average proton flux at Venus during quiet periods.

TABLE IV
SOLAR PROTON FLUX

E (keV)	0.76	1.14	1.65	2.50	3.70
$n_p v$ ($\times 10^8$ cm^{-2} sec^{-1})	1.6	2.1	2.3	2.80	0.34

The ionization rate $q(h, E)$ is proportional to the rate of energy loss dE/dh along the path of the proton, and to the proton flux $n_p v$; it is inversely proportional to the energy E_i expended per ionization. Accordingly,

$$q(h, E) = \frac{n_p v}{E_i}\frac{dE}{dh} \times \frac{10^3}{10^5} \text{ electrons cm}^{-3}\text{ sec}^{-1}, \quad (38)$$

for E_i in electron volts and h in kilometers. The rate of energy loss is

$$\frac{dE}{dh} = \frac{dE}{dw} \times \frac{dw}{dh}. \quad (39)$$

Differentiation of (37) gives

$$dE/dw = 3.37 \times 10^2 E^{0.27} \text{ keV/cm-atm}. \quad (40)$$

For an isothermal layer dw/dh is found by substitution of (11) into (14) and differentiating,

$$\frac{dw}{dh} = \frac{22.4 \times 10^3}{RT} P_b \exp\left[- \frac{mg}{RT}(h - h_b)\right]. \quad (41)$$

For a layer with a linear temperature gradient $L \neq 0$, dw/dh is found from (13) and (14),

$$\frac{dw}{dh} = \frac{22.4 \times 10^3}{RT_b} \times P_b\left[\frac{T_b}{T_b + L(h - h_b)}\right]^{(mg/RL)+1}. \quad (42)$$

Multiplication of Eq. (40) by Eq. (41) or Eq. (42), depending upon the model atmosphere being considered, and substitution into Eq. (38) yields the ionization rate for a monoenergetic beam of protons. The total ionization rate $q(h)$ may then be found by summing over the proton energy spectrum. Adopting a value of 30 eV/ionization for E_i and inserting numerical values for the constants, we find for the isothermal layer

$$q(h) = 3.02 \frac{P_b}{T} \sum_j (n_p v)_j E_j^{0.27} \times \exp\left[- \frac{mg}{RT}(h - h_b)\right], \quad (43)$$

and, for a linear temperature gradient,

$$q(h) = 3.02 \frac{P_b}{T_b} \sum_j (n_p v)_j E_j^{0.27} \times \left[\frac{T_b}{T_b + L(h - h_b)}\right]^{(mg/RL)+1}, \quad (44)$$

where the summations may be carried out for all values $h \geq h_{j,min}$ the minimum altitude to which protons of energy E_j can penetrate. The minimum altitude of penetration, obtained by equating Eq. (14) and Eq. (37), substituting the proper expression for $P(h)$, and solving for $h = h_{j,min}$ is

$$h_{j,min} - h_b = \frac{T_b}{L}\left[\left(\frac{6.34 \times 10^3 P_b}{mE_j^{0.73}}\right)^{RL/mg} - 1\right], \quad (45)$$

for the linear temperature gradient, and

$$h_{j,min} - h_b = \frac{RT}{mg} \ln\left(\frac{6.34 \times 10^3 P_b}{mE_j^{0.73}}\right), \quad (46)$$

for the isothermal layer.

Model atmospheres based upon the above equations have been constructed to examine the rate of electron production on Venus by the impact of solar protons. The models presented here have been developed subject to the constraint that most of the proton energy is depleted in ionizing the particular atmospheric region of interest, a procedure which maximizes the derived local electron densities. In the case of the isothermal models this constraint determines the pressure P_b at the base of the isothermal layer. From Table III it is seen that 3.7 keV protons penetrate to 0.0106 cm-atm. Sub-

stitution of this value into Eq. (14) yields the base pressure

$$P_b = P(h_{min}) = 4.75 \times 10^{-7}\, mg \text{ dynes cm}^{-2}. \tag{47}$$

In the case of a linear temperature gradient the above constraint was used to determine the temperature gradient L. If it is desired to produce electrons at a mean temperature $\bar{T}_e$ then the majority of the protons should be thermalized near the level in the atmosphere where $T = \bar{T}_e$. (In this and the above discussion it is assumed that the electrons are quickly thermalized. This assumption will be discussed in some detail later.) From Table III a weighted mean value of proton penetration is 0.006 cm-atm. Substitution of this and (15) into (14) gives

$$2.68 \times 10^{-7} = \frac{P_b}{mg}\left[\frac{T_b}{T_b + L(h - h_b)}\right]^{(mg/RL)}. \tag{48}$$

By taking T_b and P_b to be the temperature and pressure at the occultation level and by substitution of T_e for $T_b + L(h - h_b)$, Eq. (48) may be solved for L.

Figures 1 through 4 show the ionization curves obtained for several model atmospheres. The constant parameters for the models with a temperature gradient are $T_0 = 203°\text{K}$, $P_0 = 2.6$ dynes cm^{-2}, while the variables are T and m. For the isothermal models the ratio T/m is the variable parameter. It is obvious from these figures that increasing the temperature increases the thickness of the layer of electron formation and decreases the maximum ionization rate. The jagged or multilayered appearance of the curves results from treating the Mariner 2 flux data as five discrete monoenergetic proton fluxes. In reality the proton spectrometer accepted a fairly broad energy band ΔE for each value of E/Q measured. It is expected that proper weighting of the observed flux by the effective slit function and smoothing of the spectrum to account for those energies falling between the array of fixed slits (and not subsequently observed) would lead to a smooth ionization rate falling within the envelope defined by the extreme points in the figures.

Defining Q as the integral of the ionization rate over altitude

$$Q = \int q(h)\, dh, \tag{49}$$

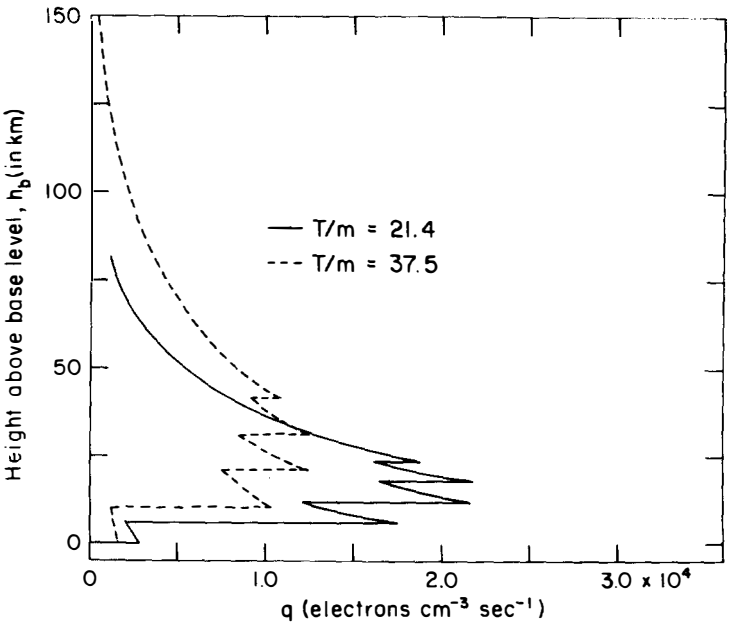

FIG. 1. Ionization rate profile due to solar protons measured by Mariner 2, for an isothermal layer with temperature, T, and mean molecular mass m, as shown.

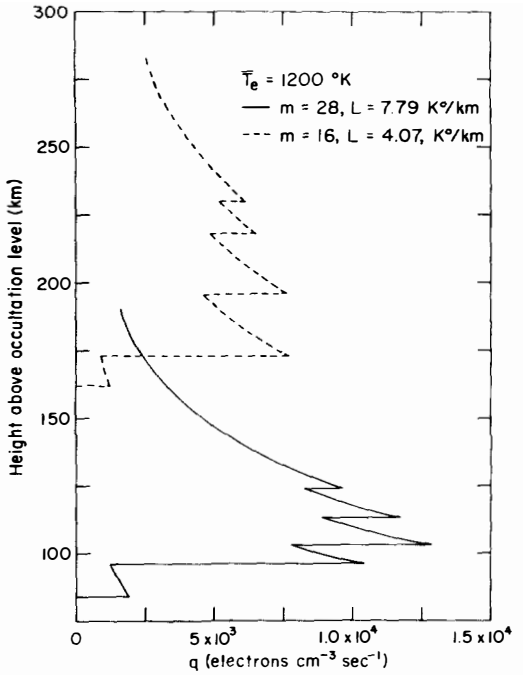

FIG. 2. Ionization rate profile due to solar protons measured by Mariner 2, for a layer with linear temperature gradient L, mean electron temperature $\bar{T}_e$, and mean molecular mass m, as shown.

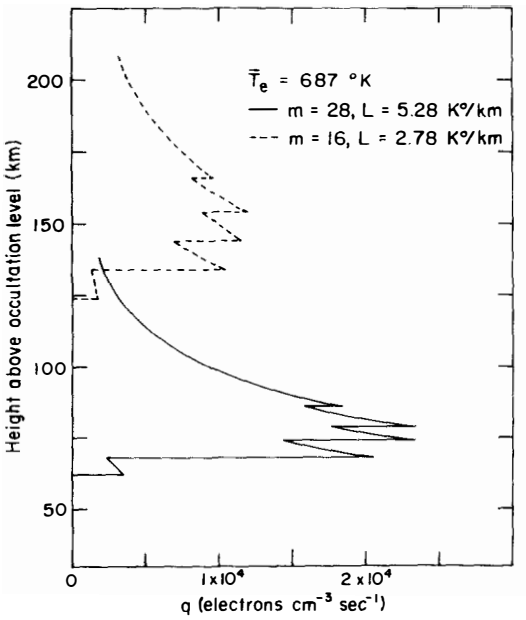

FIG. 3. Ionization rate profile due to solar protons measured by Mariner 2, for a layer with linear temperature gradient L, mean electron temperature $\bar{T}_e$, and mean molecular mass m, as shown.

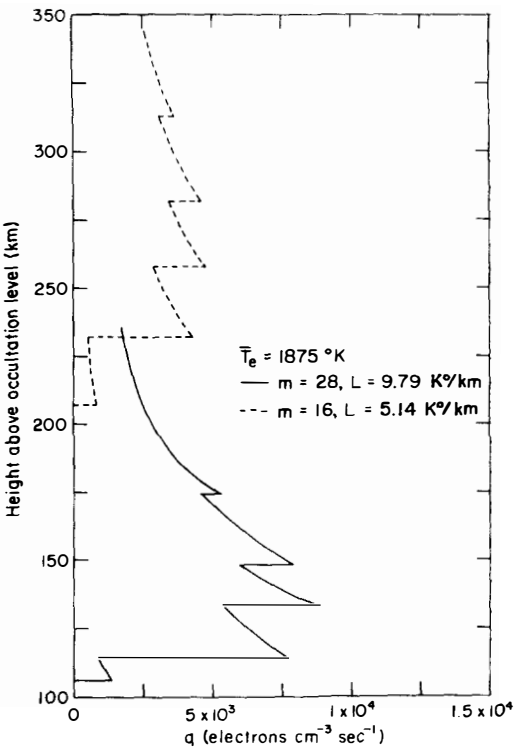

FIG. 4. Ionization rate profile due to solar protons measured by Mariner 2, for a layer with linear temperature gradient L, mean electron temperature $\bar{T}_e$, and mean molecular mass m, as shown.

we find from (30) that, at equilibrium,

$$\int q(h)\,dh = \int \alpha_e(h) n_e(h)^2\,dh, \qquad (50)$$

which, for $\alpha_e(h) = \alpha_e$ = constant, gives

$$Q = \alpha_e \int n_e(h)^2\,dh. \qquad (51)$$

Q may be determined from integration of Eq. (38) and summation over the proton flux

$$Q = \frac{10^{-2}}{E_i} \sum_j \int_{h_j}^{\infty} (n_p v)_j \left(\frac{dE}{dw}\right)_j \left(\frac{dw}{dh}\right) dh, \qquad (52)$$

$$Q = 4.6 \times 10^5 \sum_j (n_p v)_j E_j, \qquad (53)$$

a quantity which is independent of the atmospheric model. Substitution of the values of the adopted proton flux into Eq. (53) yields $Q = 7.12 \times 10^{10}$ cm^{-2} sec^{-1}.

A quantity useful for calculating the total opacity of the electron layer is

$$\Xi = \int q(h)T_e(h)^{-3/2}\,dh, \tag{54}$$

which for an ionized layer in equilibrium, by Eq. (30), is

$$\Xi = \int \alpha_e(h)T_e(h)^{-3/2}n_e(h)^2\,dh, \tag{55}$$

and for $\alpha_e(h) = \alpha_e$ = constant,

$$\Xi = \alpha_e \int T_e(h)^{-3/2}n_e(h)^2\,dh. \tag{56}$$

For the isothermal model

$$\Xi = QT_e^{-3/2} = 7.12 \times 10^{10}T_e^{-3/2}\ \text{cm}^{-2}\,\text{sec}^{-1}, \tag{57}$$

and for the linear temperature gradient integration of Eq. (38) after dividing by $T_e(h)^{3/2}$ yields

$$\Xi = \frac{1.37 \times 10^3}{[\frac{3}{2}(RL/mg) + 1]E_iT_b^{3/2}} \times \left(\frac{1.81 \times 10^{-7}mg}{P_b}\right)^{3RL/2mg} \times \sum_j (n_pv)_jE_j^{1+1.095(RL/mg)}. \tag{58}$$

As it pertains to the total opacity, a mean or effective electron temperature $\bar{T}_e$ may be defined by

$$\bar{T}_e^{-3/2} \int q(h)\,dh = \int T_e(h)^{-3/2}q(h)\,dh, \tag{59}$$

which is useful where $\alpha_e(h) \simeq \alpha_e$.

Values of the chosen parameters m, T_e, and the derived quantities L, $\bar{T}_e$, and Ξ are presented in Table V, for the linear models along with the maximum ionization rate q_m. The empirical relation

$$q_m = 5.5 \times 10^5 m/\bar{T}_e\ \text{cm}^{-3}\,\text{sec}^{-1} \tag{60}$$

derived from the table holds to within a maximum error of 7%.

Similarly, values characteristic of the isothermal models are presented in Table VI. The height of the base of the isothermal region above the occultation level, $h_b - h_0$, was calculated assuming a linear temperature gradient from the occultation level to the isothermal region. The values of Table VI fit the empirical relation

$$q_m = 4.7 \times 10^5 m/\bar{T}_e\ \text{cm}^{-3}\,\text{sec}^{-1}. \tag{61}$$

TABLE V

CHARACTERISTICS OF MODEL IONOSPHERES WITH A LINEAR TEMPERATURE GRADIENT

m	L (K°/km)	T_e (°K)	$\bar{T}_e$ (°K)	q_m (cm^{-3} sec^{-1})	Ξ (cm^{-2} sec^{-1})
28	6.54	600	688	2.34×10^4	3.94×10^6
28	4.76	1000	1210	1.29	1.69
28	3.99	1500	1890	0.88	0.87
28	3.62	2000	2550	0.60	0.55
16	7.04	600	686	1.19	3.95
16	5.10	1000	1182	0.76	1.74
16	4.26	1500	1860	0.47	0.89
16	3.86	2000	2520	0.36	0.55
35	6.32	600	682	2.72	3.98

TABLE VI

CHARACTERISTICS OF THE ISOTHERMAL MODELS

T_e (°K)	m	H (km)	q_m (cm^{-3} sec^{-1})	Ξ (cm^{-2} sec^{-1})	$h_b - h$ (km)
600	28	20.5	2.17×10^4	4.84×10^6	68
1050	28	37.5	1.25	2.09	96
600	16	37.5	1.25	4.84	131

PHOTOIONIZATION ON VENUS

For purposes of comparison with the ionization due to solar protons; it is of interest to obtain an order-of-magnitude estimate of the ionization rate due to solar ultraviolet radiation. The rate of photoionization q_p for radiation in the zenith is given by

$$q_p = \int F_\nu\sigma_\nu n\,d\nu, \tag{62}$$

where F_ν is the ultraviolet flux at frequency ν, σ_ν is the cross section for photoionization, and n is the number density of particles of cross section σ_ν. The maximum rate of ionization will occur at optical depth unity in an isothermal layer of depth given by Eq. (33). For monochromatic radiation at the top of the atmosphere of flux $F_{\nu 0}$,

$$F_\nu = F_{\nu 0}e^{-\tau_\nu}. \tag{63}$$

The maximum rate of ionization, q_m, is

$$q_m = \sigma_\nu(\mathrm{X}) n(\mathrm{X}) F_{\nu 0} e^{-1}, \qquad (64)$$

which, by virtue of Eqs. (26) and (33), with $g = 870$ cm sec^{-2}, becomes

$$q_m = 3.9 \times 10^{-6}[m(\mathrm{X})/T] F_{\nu 0} \text{ cm}^{-3} \text{ sec}^{-1}. \qquad (65)$$

Solution of Eq. (65) with $T = 1000°$K for N, N_2, O, and O_2 yields $q_m = 7600$, 15 000, 6200, and 25 000 electrons cm^{-3} sec^{-1} at $w_1 = 0.0034$, 0.0015, 0.011, and 0.0074 cm-atm, respectively. Depending somewhat upon the degree of dissociation of N_2 the ionization maxima for N and N_2 will fall within the region of significant proton ionization (see Table III). Due to the probable small abundance of O and O_2 the maxima for these ionization rates will most likely fall near or below the occultation level. [The values for the ionization cross sections and the solar ultraviolet flux were taken from Nawrocki and Papa (1961). The solar flux was increased a factor of 2 for Venus.]

A generous upper limit for the number of electrons formed per cm^2 column may be obtained by assuming that all photons effective in producing ions each produce one electron; that is,

$$\int_0^\infty q_p(h)\, dh = \int_{\nu 0}^\infty F_{\nu 0} d\nu, \qquad (66)$$

where ν_0 is the low-frequency limit for photoelectron production. Equation (66) has been evaluated in three parts, corresponding to regions effective in ionization of N + N_2, O, and O_2, respectively, since the great difference in altitude of ion formation leads one to expect considerably different values of the recombination coefficient for each region. Substituting numerical values in order gives $\int q_p(h)\, dh = [1.8 \times 10^{11} + 1.4 \times 10^{11} + 2 \times 10^{11}]$ cm^{-2} sec^{-1}.

The formation of an ionosphere is considerably more complicated than presented here. It should be emphasized that the quantities derived in this section are correct only to order of magnitude. It is, however, of interest to note that the derived quantities are of the same order as those due to the solar proton flux.

The Effective Recombination Coefficient

In general, electrons and ions can recombine by the following processes:

Radiative recombination (atomic ions)

$$\mathrm{X}^+ + \mathrm{e} \rightarrow \mathrm{X}' + h\nu \qquad (\mathrm{m})$$

Dielectronic recombination (atomic ions)

$$\mathrm{X}^+ + \mathrm{e} \rightarrow \mathrm{X}'' \rightarrow \mathrm{X}' + h\nu \qquad (\mathrm{n})$$

Dissociative recombination (molecular ions)

$$\mathrm{XY}^+ + \mathrm{e} \rightarrow \mathrm{X}' + \mathrm{Y}' \qquad (\mathrm{p})$$

Three-body recombination

$$\mathrm{X}^+ + \mathrm{e} + \mathrm{Y} \rightarrow \mathrm{X} + \mathrm{Y} \qquad (\mathrm{r})$$

or

$$\mathrm{XY}^+ + \mathrm{e} + \mathrm{Z} \rightarrow \mathrm{XY} + \mathrm{Z}, \qquad (\mathrm{s})$$

where the prime denotes that the atom or molecule is in an excited state. The double prime indicates an excited state lying in the continuum. A discussion of these processes is given by Nawrocki and Papa (1961), whose tabulated rate coefficients are adopted in the following discussion.

Radiative recombination coefficients α_r measured for atomic oxygen vary from 3.4×10^{-12} cm^3 sec^{-1} at $T = 250°$K to 0.8×10^{-12} cm^3 sec^{-1} at $T = 2000°$K. Since the major contribution to the coefficient is due to captures into excited states, it is likely that similar values will apply to nitrogen radiative recombination.

Rate coefficients for dielectronic recombination are probably on the order of 10^{-10} to 10^{-12} cm^3 sec^{-1}; however, only meager data is available on this process.

Dissociative recombination coefficients α_d for N_2^+ have measured values which range from 1.4×10^{-7} cm^3 sec^{-1} to 8.5×10^{-7} cm^3 sec^{-1} at room temperature, and 1.4×10^{-6} cm^3 sec^{-1} at $T = 2500°$K. It seems that for the present discussion a value of 10^{-7} cm^3 sec^{-1} is a conservative choice. Values for O_2^+, NO^+, CO_2^+, and H_2O^+ are all about 10^{-7} cm^3 sec^{-1} with an uncertainty of ± 2 in the exponent.

Three-body rate coefficients, β, have typical values of 5×10^{-27} cm^6 sec^{-1} for N_2^+ and O_2^+ and $10^{-26\pm2}$ cm^6 sec^{-1} for other reactions involving molecules. Similar values are attained for three-body recombination of atomic ions.

From the data of Tables IV and V it is seen that the maximum depth of proton penetration is 0.01 cm-atm for the models considered. This depth thus forms the lower boundary to the proton ionization layer. At this level Eq. (26) becomes

$$n_n(h_{min}) = 2.8 \times 10^{12} m/T, \qquad (67)$$

which for the range of m/T considered in the models yields a neutral particle number density at the lower limit of proton ionization in the range 2×10^{11} cm^{-3} to 8×10^{10} cm^{-3}.

With the aid of Eq. (34) we may compare the three-body recombination rate to that of radiative recombination. Three-body recombinations will dominate if, for $n_i = n_e$, the total particle density $N \gg \alpha_r/\beta$. From the above discussion $\alpha_r/\beta \sim 10^{15}$ cm^{-3}; thus for three-body reactions to be important N must be $\gg 10^{15}$ cm^{-3}. It should be recalled that N at the occultation level is about 10^{14} cm^3. One may conclude then that *three-body electron–ion recombination processes are not effective above the occultation level.*

The rate of radiative recombination depends upon the number density of atoms $n(\mathrm{A})$, while that for dissociative recombination on the number density of molecules $n(\mathrm{M})$. If we neglect ion–atom interchange, we may compare these rates by

$$\frac{\text{Radiative recombination rate}}{\text{Dissociative recombination rate}} = \frac{\alpha_r n(\mathrm{A}) n_e}{\alpha_d n(\mathrm{M}) n_e}. \qquad (68)$$

These rates are equal for $n(\mathrm{A})/n(\mathrm{M}) = \alpha_d/\alpha_r \sim 10^5$. It is apparent that a very high degree of dissociation is required for radiative recombination to be important. A similar conclusion may be reached concerning dielectronic recombination, although if the rate coefficient can be as large as 10^{-10} cm^3 sec^{-1} the rates of dielectronic and dissociative recombination would be equal for $n(\mathrm{A})/n(\mathrm{M}) \sim 100$, a much smaller degree of dissociation.

To achieve this high degree of dissociation with the assumed large abundance of N_2 requires that the Herzberg-Herzberg mechanism be very efficient. This requires a low abundance of H, H_2, O_2, O_3, and NO since these molecules have moderate to strong absorptions in the region 1200–1250Å. Collisional frequencies of molecules and atoms in the region of proton ionization are on the order of 1 per sec; thus collisional de-excitation of N_2 in the "Herzberg State" prior to dissociation is unlikely (lifetime of state $\sim 10^{-3}$ sec).

The dissociation of N_2 in the terrestrial atmosphere through the Herzberg-Herzberg process is limited by diffusion (see, e.g., Bates, 1954), and it is easy to show that a similar conclusion applies to Venus. A simple solution of the one-dimensional diffusion equation yields for the diffusion current of the jth molecular species,

$$J_j \simeq -D_j(\Delta n_j/\Delta h), \qquad (69)$$

where $\Delta n_j/\Delta h$ is the concentration gradient, and

$$D_j \simeq \frac{(3kT/m_j)^{1/2}}{12\pi\, nr^2}. \qquad (70)$$

A characteristic time for the establishment of diffusive equilibrium in an isothermal region above a critical level, h_c, characterized by an overall number density n_c, and a number density n_{cj} for the jth constituent is

$$t_j = n_{cj} H_j / J_j, \qquad (71)$$

where H_j is the scale height of the jth constituent in the diffusion regime. Substitution of (69) and (70) into (71) yields for the characteristic velocity of the jth constituent, diffusing between some altitude $h = \Delta h + h_c$ where $n \ll n_c$ and the critical level, the expression

$$v_{cj} = \frac{\Delta h}{t_j} \simeq \frac{\sqrt{3}}{12\pi n_c r^2}\left(\frac{g}{H_j}\right)^{1/2}. \qquad (72)$$

Diffusive equilibrium exists when v_{cj} is much larger than the prevailing turbulent velocities. For the Earth, diffusive equilibrium is established when v_{cj} exceeds a few cm sec^{-1}.

The factors controlling the prevailing turbulent velocities in the Earth's upper atmosphere are very complicated and almost entirely unknown. Venus is a planet which is very slowly rotating. Some very simple models of the atmospheric circulation for the likely high surface pressures give prevailing wind velocities which are not excessive by terrestrial standards (Mintz, 1962). In the absence of any further information we will adopt the same value for v_{cj} for the establishment of diffusive equilibrium that prevails on Earth. The qualitative conclusions which we will later draw in this paper do not depend critically on this assumption. We then find,

$$n_c \sim 3 \times 10^{11} \text{ cm}^{-3}$$

for $H_j \sim 30$ km. This value is not sensitively dependent on the choice of H_j. Thus, diffusive equilibrium is established at about the level of proton and ultraviolet ionization, but significantly above the occultation level.

The N_2 dissociation rate through the Herzberg-Herzberg mechanism on Venus is

$$q(\text{j}) \sim 4 \times 10^{-12} n(\text{N}_2).$$

Taking the atmosphere to be primarily N_2 at the ionization level, we find there

$$q(\text{j}) \sim 0.4 \text{ cm}^{-3} \text{ sec}^{-1}.$$

The mean dissociation time is then $10^{11}/0.4 \sim 2 \times 10^{11}$ sec, or several thousand years. But the corresponding times for diffusive mixing of the atomic nitrogen photodissociation products of the Herzberg-Herzberg mechanism is, by (71), of the order of days. When the nitrogen atoms diffuse to altitudes where the total number density is 10^{11} or 10^{12} cm^{-3}, they rapidly recombine (see, e.g., Bates, 1954) by the three-body process (l). Accordingly, the Herzberg-Herzberg mechanism is generally inefficient on Venus; molecular nitrogen will be abundant at the ionization level; and dissociative recombination cannot be avoided.

We conclude that the effective recombination coefficient near the region of maximum ionization in the upper Cytherean atmosphere is

$$\alpha_e \sim 10^{-7} \text{ cm}^3 \text{ sec}^{-1}. \tag{73}$$

Calculation of the ionization rate by protons involved the assumption that the electron temperature was equal to the local kinetic temperature. The validity of this assumption will now be examined. The time t for electrons ejected with excess energy U (electron volts) to thermalize at temperature T is given by Ginzburg (1961) as

$$t = \frac{\ln (U/kT)}{\nu_e \delta} \text{ sec}, \tag{74}$$

where k is Boltzmann's constant and for elastic collisions in atomic gases $\delta = 1.088 \times 10^{-3} A$, A being the atomic weight of the particles. For inelastic collisions in air and similar molecular mixtures $\delta \sim 10^{-3}$ [see Ginzburg (1961), Table 5.1, p. 69 for exact values].

From Eq. (29) the average lifetime of an ion is $\Delta t = (N_i \alpha_e)^{-1}$ sec, where N_i is the number density of ions. If $\Delta t > t$ the electrons will have time to thermalize and $T_e = T$; thus for electrons to thermalize we require

$$\alpha_e < \frac{\nu_e \delta}{n_i \ln (U/kT)}. \tag{75}$$

It can be easily shown that for $n_n < 2 \times 10^6 n_i$, Eq. (22) determines ν_e. Substitution of (22), $\delta = 10^{-3}$, and $U = E_i$ — Ionization potential ~ 15 eV yields the requirement that $\alpha_e < 2 \times 10^{-7}$ cm^3 sec^{-1}. Since the deduced value of α_e is 10^{-7} cm^3 sec^{-1} the assumption $T_e = T$ is approximately valid.

Results and Conclusions

From the results displayed in Tables V and VI, it is seen that the maximum rates of ionization consistent with the observed proton spectrum are $\sim 2 \times 10^4$ cm^{-3} sec^{-1}, while the upper values of Ξ are $\sim 5 \times 10^6$ cm^{-2} sec^{-1}. From Eqs. (51) and (53), we find $\int n_e^2 \, dh \sim 7 \times 10^{17}$ cm^{-5} for $\alpha_e \sim 10^{-7}$ cm^3 sec^{-1}. In all our proton ionization models, the ionized layers are $\sim$50 km thick (cf. Figs. 1–4). The corresponding mean electron density is $\sim 4 \times 10^5$ cm^{-3}. Photoionization will contribute an electron density of the same order of magnitude. Had radiative recombination and $\alpha_e \sim 10^{-12}$ cm^3 sec^{-1} been realizable, values of $\int n_e^2 \, dh$ approaching 10^{23} cm^{-5} and values of $n_e \sim 10^8$ cm^{-3} would

have been derived. Even these electron densities are too low for the ionospheric model. But because of the great abundance of N_2 in the region where ionization occurs, values of n_e even as large as 10^7 cm^{-3} are excluded.

For $\Xi = 5 \times 10^6$ cm^{-2} sec^{-1} and $\alpha_e = 10^{-7}$ cm^3 sec^{-1}, the optical depth of the ionized layer, due to free–free emission, would be, from Eqs. (9) and (56), $\tau(\lambda) \sim 4 \times 10^{-9}\ \lambda^2$. Significant opacity occurs only for $\lambda > 100$ meter, far beyond the microwave region of relevance for Venus. Had we chosen $\alpha_e \sim 10^{-12}$ cm^3 sec^{-1}, we would have found $\tau(\lambda) \sim 4 \times 10^{-4}\ \lambda^2$, implying $\tau(10\text{ cm}) = 0.04$, and $\tau(68\text{ cm}) = 1.8$. Even these optical depths are inadequate to explain the microwave observations by free–free emission, although they would have caused significant attenuation of long-wavelength radar returns from Venus.

The models developed for the formation of a Cytherean ionosphere by solar protons assumed a vanishing magnetic field strength. It is well known that interactions between a neutral plasma and an external magnetic field are governed by the relative energy densities of the field and the plasma. If the energy density of the plasma is greater than that of the field, charge separation does not occur and the trajectories of the individual particles are governed by the plasma rather than by the magnetic field. The energy density U_p of the proton stream is

$$U_p = \tfrac{1}{2}m \sum_j n_{0j} v_j^2 = \sum_j n_{0j} E_j. \qquad (76)$$

The energy density U_m of the magnetic field is

$$U_m = B^2/8\pi. \qquad (77)$$

If we require $U_p > U_m$ the proton stream will not be appreciably deflected by the magnetic field; this condition can be written

$$B < (8\pi \sum_j n_{0j} E_j)^{1/2}. \qquad (78)$$

Substitution of numerical values from Table IV yields $B < 1.04 \times 10^{-3}$ gauss.

The Mariner 2 magnetometer experiment (Smith *et al.*, 1963) detected no sign of a Cytherean magnetic field at a distance of 4.1×10^4 km from the planet. This result, and similar negative results in the search for Cytherean radiation belts, lead to the conclusion that the magnetic moment of Venus is less than that of Earth; however, a surface magnetic field strength of 0.1 gauss is not inconsistent with the observations [see, e.g., Sonett (1963)]. The slow rotation rate of Venus, obtained from radar observations, is also consistent with a low magnetic field, but theories of the origin of the geomagnetic field are not nearly in a sufficiently satisfactory state to predict whether the Cytherean surface field strength is greater than or less than 10^{-3} gauss.

The effect of a local magnetic field on the microwave absorption coefficient and thus on the optical depth of the ionospheric layer is well known. Magnetic field effects become important when the gyrofrequency ω_H approaches the angular frequency ω of the wave; then [see, e.g., Ratcliffe (1959)] $\omega_H/\omega \sim 10^{-4}\ B\lambda$, when λ is in cm and B in gauss. For $\lambda = 68$ cm, $\omega_H/\omega = 1$ for $B = 147$ gauss, a value not admitted by the Mariner 2 observations.

Thus, no permissible combination of Cytherean magnetic field strength and atmospheric composition yields results compatible with the ionospheric model. If we refuse to invoke some other unknown ionization source, it follows that we must reject the ionospheric model. A similar conclusion was reached by Sagan, Siegel, and Jones (1961) and by Kellogg and Sagan (1961). Our maximum derived electron densities are much smaller than those required by Jones (1961), by Priester, Roemer, and Schmidt-Kaler (1962), and by Kuzmin (1964). The discussion of Danilov and Yatsenko (1963) requires that the ionospheric optical depth at 10 cm be of the order of 2, a value much larger than the known ionization sources permit.

If we were to postulate additional proton fluxes with energies outside the range measured by Mariner 2, we would be faced with the following difficulties:

1. If an additional flux of *high*-energy protons is postulated, these protons will

penetrate deeply into the atmosphere and produce most of their ionization in regions where the recombination coefficient is large, thus greatly reducing their effectiveness.
2. If a flux of low-energy particles is postulated, the required flux must be increased many orders of magnitude to make up for the loss in ionization efficiency of the low-energy protons.

The question of the proton flux at smaller energies than those measured by Mariner 2 is relevant to the observed correlation of the 68-cm radar determination of the distance to Venus with the 10.7-cm and 20-cm solar flux. No such correlation has been reported for the 12.5-cm radar ranging. Muhleman (1963) has postulated that solar activity somehow *reduces* the Cytherean electron density, temporarily increasing the group velocity of the radar pulse in the Cytherean ionosphere, and decreasing the measured value of the astronomical unit. Muhleman can match the observations if $\int n_e^2\, dz \sim 5 \times 10^{22}$ cm^{-5}, provided $n_e \sim 10^7$ cm^{-3} and $\Delta z \sim 10^4$ km. This assumed ionospheric scale height is much greater than the measured solar proton flux admits (cf. Figs. 1–4, where $\Delta z \sim 50$ km). Muhleman's explanation of the correlation between the radar range and solar activity is, therefore, admissible only if there exists an alternative ionization source—perhaps a very large flux of low-energy protons which are thermalized at very high altitudes where radiative recombination (due to O^+, for example) dominates. But even then, the admissible values of $\int n_e^2\, dz$ are inconsistent with the ionospheric model of the microwave emission, as Muhleman (1963) himself emphasized.

The foregoing difficulties with the ionospheric model lead us to conclude that the surface of Venus is the source of the observed microwave emission. Greenhouse models of Venus now appear capable of explaining the high surface temperatures and the observed microwave spectrum and phase effect (Sagan and Pollack, 1965; Pollack and Sagan, 1966).

Acknowledgment

We are grateful to Prof. David R. Bates for a critical reading of the manuscript.

References

Barath, F. T., Barrett, A. H., Copeland, J., Jones, D. E., and Lilley, A. E. (1963). Mariner II: Preliminary reports on measurements of Venus—Microwave radiometers. *Science* **139,** 908–909.

Barrett, A. H., and Staelin, D. H. (1964). Radio observations of Venus and the interpretations. *Space Sci. Revs.* **3,** 109–135.

Bates, D. R. (1954). The physics of the upper atmosphere. *In* "The Earth as a Planet" (G. P. Kuiper, ed.), pp. 576–636. Univ. of Chicago Press, Chicago, Illinois.

Bottema, M., Plummer, W., and Strong, J. (1964). Water vapor in the atmosphere of Venus. *Astrophys. J.* **139,** 1021–1022.

Brandt, J. C. (1962). A model of the interplanetary medium. *Icarus* **1,** 1–6.

Chamberlain, J. W. (1965). *Astrophys. J.* **141,** 1184–1205.

Cook, C. J., Jones, E., Jr., and Jorgensen, T., Jr. (1953). Range-energy relations of 10- to 250-keV protons and helium ions in various gases. *Phys. Rev.* **91,** 1417–1422.

Danilov, A. D. (1964). Radioastronomical research and current concepts of the atmosphere of Venus. *Kosmichoskiye Issledovaniya* **2,** 188–215.

Danilov, A. D., and Yatsenko, S. P. (1963). An ionospheric interpretation of results of radio observations of Venus. Parts I and II. *Geomagnetism and Aeronomy* **3,** 585–597.

de Vaucouleurs, G., and Menzel, D. H. (1960). Results of the occultation of regulus by Venus. *Nature* **188,** 28–33.

Drake, F. D. (1962). 10-cm observations of Venus in 1961. *Publ. Natl. Radio Astron. Obs.* **1,** 165–178.

Ginzburg, V. L. (1961). "Propagation of Electromagnetic Waves in Plasma" (W. L. Sadowski and D. M. Gallik, eds.). Gordon and Breach, New York.

Jones, D. E. (1961). The microwave temperature of Venus. *Planetary Space Sci.* **5,** 166–167.

Kellogg, W. W., and Sagan, C. (1961). The atmospheres of Mars and Venus. *Natl. Acad. Sci-Natl. Res. Council Publ.* **944** (Washington, D. C.).

Kotelnikov, V. A. (1961). Radar contact with Venus. *J. Brit. Inst. Radio Engrs.* **621,** 293–295.

Kourganoff, V. (1952). "Basic Methods in Transfer Problems." Clarendon Press, Oxford, England.

Kuzmin, A. D. (1964). On the ionospheric model of Venus. *In* "Life Sciences and Space Research, II" (M. Florkin and A. Dollfus, eds.),

pp. 211–221. North-Holland Publ. Co., Amsterdam.

MAYER, C. H. (1963). General report on planetary radio astronomy. *Proc. Intern. Astrophys. Colloq., 11th, Liege, 1963,* pp. 99–111.

MINTZ, Y. (1962). The energy budget and atmospheric circulation on a synchronously rotating planet. *Icarus* **2,** 172–173.

MINZNER, R. A., AND RIPLEY, W. S. (1957). "Handbook of Geophysics," 1st ed. Air Force Cambridge Res. Lab., Bedford, Massachusetts.

MITRA, S. K. (1952). "The Upper Atmosphere," 2nd ed. The Asiatic Society, Calcutta, India.

MUHLEMAN, D. O. (1963). The electrical characteristics of the atmosphere and surface of Venus from radar observations. *Icarus* **1,** 401–411.

NAWROCKI, P. J., AND PAPA, R. (1961). Atmospheric processes. *Air Force Cambridge Res. Lab. Rept. No.* **AFCRL-595.**

NEUGEBAUER, M., AND SNYDER, C. W. (1962). Preliminary results from the Mariner 2 solar plasma experiment. *Jet Propulsion Lab., Calif. Inst. Technol., Tech. Memo. No.* **33-111.**

ÖPIK, E. J. (1961). The aeolosphere and atmosphere of Venus. *J. Geophys. Res.* **66,** 2807–2819.

OSTER, L. (1961). Emission, absorption, and conductivity of a fully ionized gas at radio frequencies. *Rev. Mod. Phys.* **33,** 525–543.

PETTENGILL, G. H., BRISCOE, H. W., EVANS, J. V., GEHRELS, E., HYDE, G. M., KRAFT, L. G., PRICE, R., AND SMITH, W. B. (1962). A radar investigation of Venus. *Astron. J.* **67,** 181–190.

POLLACK, J. B., AND SAGAN, C. (1965). The microwave phase effect of Venus. *Icarus* **4,** 62–103.

PRIESTER, W., ROEMER, M., AND SCHMIDT-KALER, TH. (1962). Apparent relation between solar activity and the 440-Mc/s radar distance of Venus. *Nature* **196,** 464–465.

RATCLIFFE, J. A. (1959). "Magnetoionic Theory." Cambridge Univ. Press, Cambridge, England.

SAGAN, C. (1960). The radiation balance of Venus. *Jet Propulsion Lab., Calif. Inst. Technol., Tech. Rept.* **32–34.**

SAGAN, C. (1961). The planet Venus. *Science* **133,** 849–858.

SAGAN, C. (1962). Structure of the lower atmosphere of Venus. *Icarus* **1,** 151–169.

SAGAN, C., AND KELLOGG, W. W. (1963). The terrestrial planets. *Ann. Rev. Astron. Astrophys.* **1,** 235–266.

SAGAN, C., AND POLLACK, J. B. (1965). On the nature of the clouds and the origin of the surface temperature of Venus. To be published.

SAGAN, C., SIEGEL, K. M., AND JONES, D. E. (1961). On the origin of the Venus microwave emission (abstract). *Astron. J.* **66,** 52.

SMITH, E. J., DAVIS, L., COLEMAN, P. J., AND SONETT, C. P. (1963). Mariner 2: Preliminary measurements of Venus — Magnetic field. *Science* **139,** 909–910.

SONETT, C. P. (1963). A summary review of the scientific findings of the Mariner Venus mission. *Space Sci. Revs.* **2,** 751–777.

VICTOR, W. K., AND STEVENS, R. (1961). Exploration of Venus by radar. *Science* **134,** 46–48.

WHIPPLE, F. L. (1962). Quoted by Muhleman (1963).